Available online at www.sciencedirect.com

ScienceDirect

Procedia Structural Integrity 47 (2023) 337–347

Structural Integrity Procedia

www.elsevier.com/locate/procedia

27th International Conference on Fracture and Structural Integrity (IGF27)

Influence of Ni-P + DLC multilayer coatings on the tensile properties of the AlSi10Mg alloy produced by Laser-based Powder Bed Fusion

G. Di Egidio[a]*, L. Ceschini[a], C. Martini[a], A. Morri[a]

[a]*Department of Industrial Engineering (DIN), Alma Mater Studiorum, University of Bologna, Viale Risorgimento 4, 40136 Bologna, Italy*

Abstract

The peculiar microstructure of the AlSi10Mg alloy produced by the laser-based powder bed fusion (L-PBF) process requires the development of specific heat treatments and coatings to exploit its potential fully. The study aims to evaluate the effect of the deposition of an anti-friction/wear Ni-9%P + DLC (hydrogenated amorphous carbon, a-C:H) multilayer coating produced in an industrial environment by the electroless process followed by Arc-Evaporation Physical Vapor Deposition (PVD), on the mechanical properties of the L-PBF AlSi10Mg alloy. In the processing sequence, the DLC deposition phase replaces the artificial aging step in the T5 (direct aging) and T6R (solution treatment, quenching, and aging) heat treatments to reduce industrial costs thanks to comparable temperatures and soaking times. Therefore, the coated samples undergo the following post-production cycles: (i) Ni-P + DLC deposition (T5-like heat treatment) and (ii) rapid solution (SHTR) (10 min at 510 °C) + Ni-P + DLC deposition (T6R-like heat treatment). Tensile tests highlight a significant reduction in ductility for T6R-like and T5-like specimens due to the different mechanical responses under static load between the multilayer coating and the substrate. At the same time, no significant differences are found in terms of strength properties. In conclusion, the variation in the static mechanical property trade-off of L-PBF AlSi10Mg induced by this processing cycle reveals critical points to be taken into account when applying a multilayer coating to structural components.

Keywords: Laser-based Powder Bed Fusion (L-PBF); AlSi10Mg; tensile test; Diamond-like Carbon (DLC); Electroless Ni-P coating.

* Corresponding author.
E-mail address: gianluca.diegidio2@unibo.it

10.1016/j.prostr.2023.07.091

1. Introduction

Al alloys have found widespread applications in the automotive and aerospace sectors due to their excellent properties, such as high strength-to-weight ratio, high thermal conductivity, and good corrosion resistance. However, the production of complex-shaped components can lead to manufacturing issues when traditional subtractive manufacturing methods are used. The laser-based powder bed fusion (L-PBF) process has proven capable of producing custom-designed components using a layer-by-layer deposition strategy, suiting industrial sectors with a low production volume of high-value-added parts. Additionally, the L-PBF process reduces the total number of components via the Design for Additive Manufacturing (DAM) approach, thus lowering manufacturing cost and risk of failure, improving the component's performance by a higher strength-to-weight ratio and reducing material usage as the complexity of the part increases. For these reasons, aerospace and automotive industries have adopted L-PBF-produced components on a large scale, transitioning from rapid prototyping into mass production [1,2].

Currently, the Al-Si hypoeutectic alloys represent the most widely used and studied Al alloys for L-PBF printing (mostly with 7 - 12 wt% Si and up to 0.6 wt% Mg) as a narrow solidification range characterizes the almost eutectic composition, which reduces the hot cracking susceptibility. In particular, the AlSi10Mg alloy has received the most industrial and academic attention within the Al-Si family due to its excellent balance between mechanical properties and printability [3].

Among non-ferrous alloys, Al alloys constitute the largest group of substrates suitable for electroless nickel (Ni-P) plating, improving the hardness and resistance to abrasion, wear, and corrosion of these alloys [4]. Engine piston represents a successful combination of Al-Si substrate and Ni-P: lightweight moving components work more efficiently, while Ni-P coating provides wear resistance to extend the useful life [5].

To further enhance the tribological properties of the L-PBF AlSi10Mg alloy, a Diamond-like Carbon (DLC) coating, characterized by high hardness and surface quality, low friction coefficient, and good wear resistance, can be applied as the top coating of the Ni-P interlayer [6]. In particular, the hydrogenated amorphous carbon (a-C:H) form has been widely used in the past few years to reduce contact friction [7]. However, hard DLC coatings should not be directly deposited on a soft substrate such as AlSi10Mg unless an interlayer, such as the Ni-P coating, is deposited [8]. Furthermore, high residual stresses in the DLC coating may promote delamination phenomena and low durability, not allowing the deposition of thick films (maximum 2 - 3 μm).

Even though the literature has reported the advantages of multilayer coatings on the tribological properties of Al alloys [5-11], a small number of investigations have been conducted on the effects of overlay coatings on the tensile properties [4,12-14], and none on the innovative L-PBF AlSi10Mg alloy. Considering the high mechanical stress to which Al-based structural components are subjected, it is essential to know how the mechanical properties of parts change in coated and uncoated conditions.

The present work analyzes the integration of the Ni-9%P + DLC multilayer coating deposition into a heat treatment cycle, obtaining good mechanical performance and reducing industrial time and costs. In particular, DLC deposition replaces the artificial aging (AA) step based on comparable treatment temperatures and times. Therefore, the study performs mechanical and fractographic characterization of the L-PBF AlSi10Mg alloy subjected to two different integrated cycles: (i) T5-like heat treatment, consisting of the Ni-P + DLC deposition; (ii) T6R-like heat treatment, i.e., Ni-P deposition, followed by a rapid solution (SHTR) at 510 °C for 1 h, optimized in previous work [15], and DLC deposition to induce the precipitation hardening.

2. Experimental procedure

2.1 Samples production

An industrial SLM500 printing system produced vertical rod specimens (diameter of 9 mm and height of 77 mm) into a building chamber filled with high-purity Ar gas (O_2 level below 0.2 vol.%), using the following process

parameters: (i) laser power: 350 W, (ii) scan rate: 1150 mm/s, (iii) layer thickness: 50 µm, (iv) hatch distance: 170 µm, and (v) heated platform: 150 °C. The printing process took about 30 h. A bidirectional stripe scan strategy and a 67° counter-clockwise rotation between subsequent layers were adopted. Further information about the powder physical properties and chemical composition are reported in [15].

2.2 Integrated cycles

The study aims to develop integrated post-process cycles for the L-PBF AlSi10Mg alloy consisting of heat treatment and coating deposition. The aim of the two heat treatments is different: (i) maximizing the mechanical strength and reducing residual stress (T5-like) and (ii) increasing the strength-to-ductility trade-off (T6R-like). More details on heat treatment optimization can be found in our previous works [15,16]. In this study, the DLC deposition replaced the AA phase in both heat treatments to reduce post-processing time and cost. Therefore, two integrated cycles were designed, T5-like and T6R-like (Figure 1), used respectively to obtain coated samples, hereafter referred to as T5-C and T6R-C, and uncoated samples, hereafter referred to as T5-U and T6R-U, useful for the comparison.

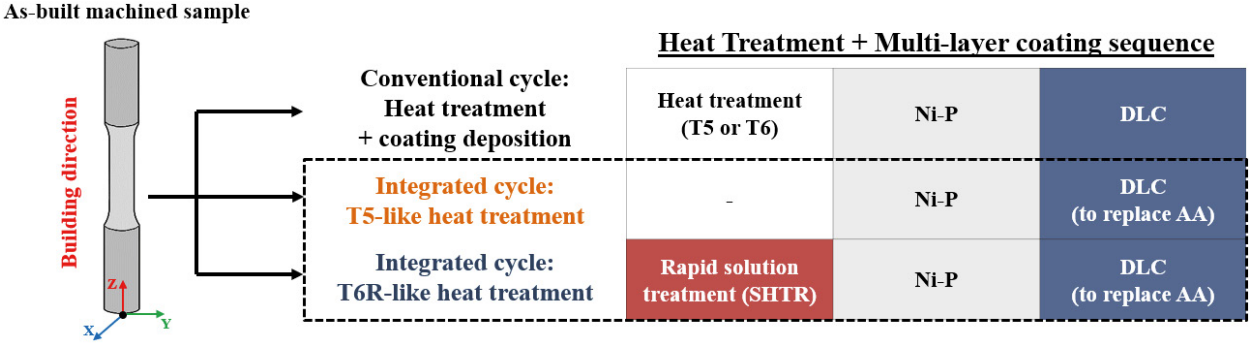

Fig. 1. Industrial cycle explored in this research compared to the conventional industrial procedure. The load axis of the tensile specimen is parallel to the building direction (z-axis) to increase the number of components on a single platform. SHTR: rapid solution at 510 °C for 10 min; AA: artificial aging.

Round dog-bone tensile samples (gauge length L_0 = 25 mm, gauge diameter d_0 = 5 mm) (Figure 1) were machined from the as-built (AB) specimens and subjected to the deposition coating sequence (Ni-P and DLC). Only the T6R-like specimens were SHTRed before the deposition sequence. SHTR step was carried out in an electric furnace with a temperature control of ± 5 °C. Medium Ni-P coating (9 wt.% P) was deposited in an industrial facility at temperatures lower than 100 °C; consequently, the effects on the microstructure of the substrate are negligible considering the temperature of the heated platform (150 °C) and the printing time (30 h). For the T6R alloy, Ni-P deposition occurred post-SHT step to avoid the formation of thin Ni oxide and consequent problems during the DLC coating deposition using the Arc-Evaporation Physical Vapor Deposition (PVD) process.

2.2 Mechanical characterization

HV_1 hardness and tensile tests were performed on T5-like and T6R-like. In particular, hardness tests were performed to check the substrate condition post-deposition cycle and compare it with the aging curves reported in a previous study on the L-PBF AlSi10Mg alloy [15]. Tensile tests were carried out at room temperature on a screw-testing machine at a strain rate of 3.3×10^{-3} s^{-1} according to DIN EN ISO 6892-1:2020. Yield Strength (YS), Ultimate Tensile Strength (UTS), and elongation to failure (e_f) were evaluated as the average of at least three samples for each investigated condition.

2.3 Microstructural and fractographical analysis

Cross-sections for microstructural analysis were extracted from tensile specimens, embedded in conductive resin, grounded, and finally polished with diamond suspensions up to 1 µm, according to ASTM E3-11(2017). Then, they were etched with Weck's reagent (3g NH_4HF_2, 4 mL HCl, 100 mL H_2O) according to ASTM E407-07(2015).

Microstructural analyses were carried out by MIRA3 FEG-SEM (TESCAN, Brno, Czech Republic) with Energy-Dispersive X-ray Spectroscopy (EDS, Brucker Quantax 200/30 mm^2, Billerica, Massachusetts, US). At the same time, fractographic analyses were carried out to assess the coating and substrate failure mechanisms using a multi-focus 3D-digital microscope (HIROX, Tokyo, Japan) and MIRA3 FEG-SEM.

3. Results

3.1. Effect of DLC deposition on substrate hardness

The DLC coating was deposited in an industrial facility where the temperature is not measured directly on the specimens. Therefore, identifying the thermal exposure effects during the DLC deposition on the L-PBF AlSi10Mg alloy is fundamental for verifying the feasibility of substituting the AA in the integrated cycle.

After T5-like heat treatment (Ni-P + DLC deposition), the substrate is characterized by a hardness equal to 130 ± 2 HV_1. In contrast, after T6R-like heat treatment (SHTR + Ni-P + DLC deposition), the value decreases to 91 ± 4 HV_1. By comparing with the aging curves reported in [14] (Figure 2), the specimens may have been subjected to thermal exposure during the DLC deposition, equivalent to 4 - 5 h at 180 °C. As a result, the coating deposition conditions promote alloy overaging compared to optimized AA conditions [14].

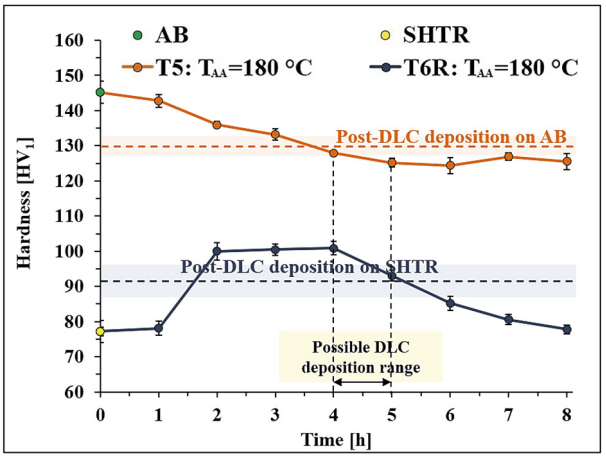

Fig. 2. Artificial aging curves carried out on AB alloy (T5-like) and after SHTR treatment (T6-like) (adapted from [14]). The thick dotted lines indicate average hardness values measured on the substrate after the NI-P+DLC deposition. The colored bands show the standard deviation.

3.2 Microstructural characterization

EDS analysis shows that the Ni-P interlayer's average P content is 9.3 wt.%. Therefore, this coating can be classified as "medium phosphorus" [17]. As reported in the literature [12,18], this P content results in amorphous microstructure, higher hardness, and smoother surface roughness compared to lower P deposits and a compressive residual stress state. Furthermore, the Ni-P coating is characterized by a thickness equal to 16.5 ± 1.5 µm and good adhesion to the substrate (Figure 3). A Cr-W bond layer (1.5 ± 0.1 µm) is used to improve the adhesion between the Ni-P interlayer and DLC top-coating (1.3 ± 0.1 µm). The substrate shows typical heat-treated L-PBF AlSi10Mg microstructure: (i) submicrometer α-Al cells surrounded by a eutectic-Si fibrous network for T5-like heat-treated alloy (Figure 3(a)), and (ii) homogeneous distribution of spheroidal Si particles embedded into Al matrix for T6R-heat-treated like alloy (Figure 3(b)).

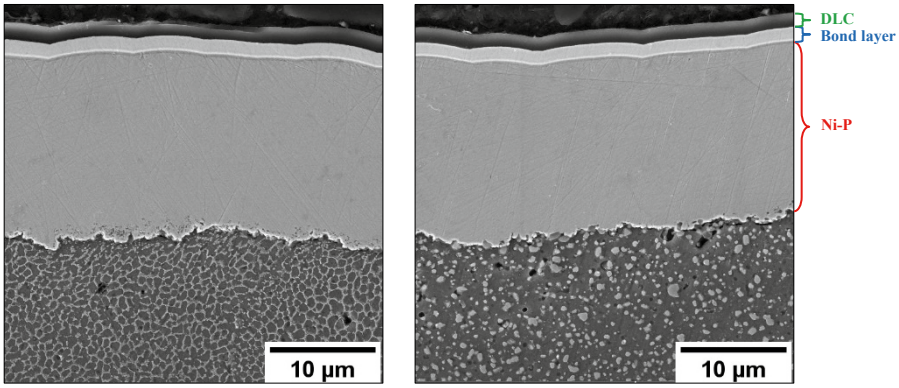

Fig. 3. Detail of the superficial zone of the T5-like (a) and T6R-like (b) specimens.

T5-like and T6R-like heat treatments do not induce significant or macroscopical modification of the substrate microstructure (Figure 4). Therefore, the slight decrease in hardness observed after coating deposition is due to the coarsening of strengthening precipitates (nano-sized Si particles and Mg_2Si precursor phases) induced by diffusion phenomena [19]. n particular, the coarser reinforcing precipitates that form with increasing thermal exposure (temperature or steep time) offer lower resistance to dislocation motion, thereby reducing the hardness of the heat-treated alloy.

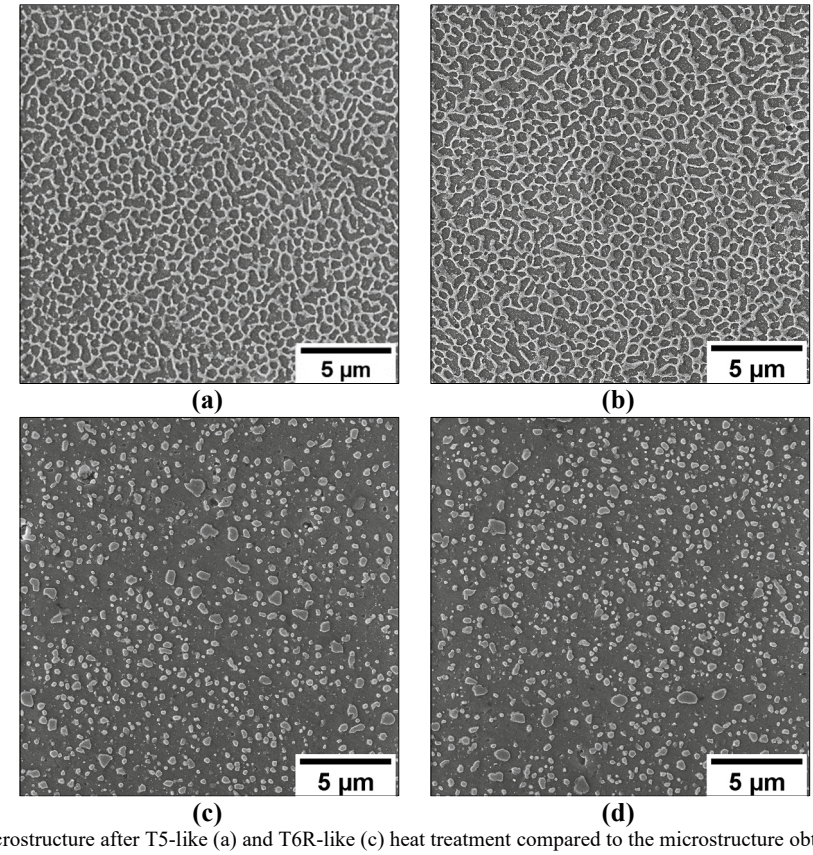

Fig. 4. Detail of the microstructure after T5-like (a) and T6R-like (c) heat treatment compared to the microstructure obtained after optimized T5 (b) and T6R (d) heat treatment reported in [14].

3.3 Tensile test

Tensile behavior was evaluated on coated (T5-C and T6R-C) and uncoated (T5-U and T6R-U) samples, which were polished to remove the multilayer coating to perform the tensile tests on samples subjected to the same thermal exposure. Tensile properties (YS, UTS, and e_f) are reported in Figure 5.

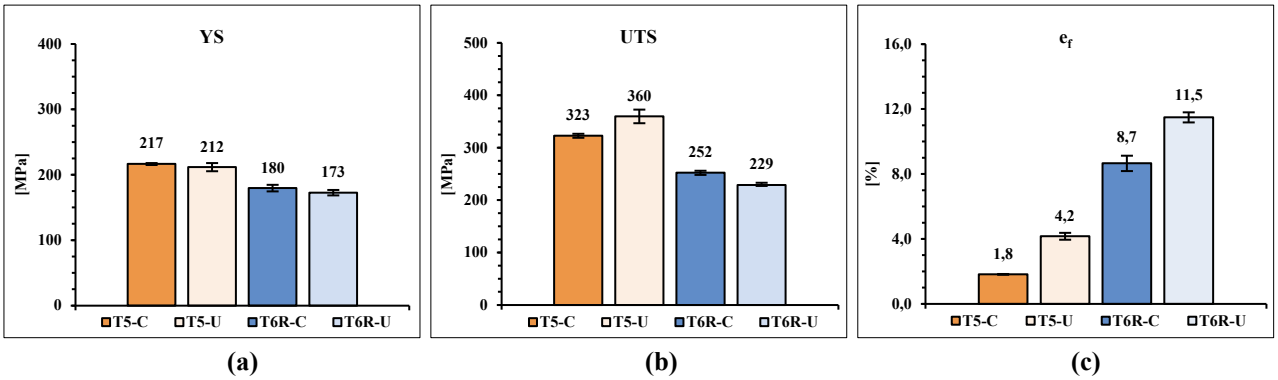

Fig. 5. Tensile properties (YS (a), UTS (b), and e_f (c)) of the T5 and T6R alloy tested in different conditions: (i) coated (T5-C and T6R-C), (ii) uncoated (T5-U and T6R-U). The T-bars represent standard deviations.

As can be appreciated by Figure 5, the multilayer coating slightly modifies the strength properties. YS remains almost unchanged, while UTS is higher in T6R-C (about 10%) but lower in T5-C (about 10%). The Ni-P coating has higher tensile properties than Al alloys, and, as observed in other coated Al alloys [4,12,13], it can increase the strength properties of the system, as occurs in the T6R-C alloy [20]. Conversely, in the T5-C alloy, severe damage originates from the eutectic-Si network at a low strain since the Si phase is interconnected and can not accommodate high strain before failure [21]. In this heat-treated condition, this feature of the Si network can lead to incipient failure at the substrate/interlayer interface and a significant reduction in UTS due to the absence of necking phenomena [15].

Furthermore, the as-deposited Ni-P interlayer has an amorphous structure characterized by limited ductility [22,23] and can sustain only a limited plastic deformation (e_f value of 1 - 1.5%) [13,14]: as load exceeds YS value, it is more difficult for the multilayer coating to accommodate the Al substrate strain. Therefore, cracks form at the Ni-P/Al interface [24] and propagate during substrate plastic deformation, leading to a premature failure of the coated samples. The results support this consideration, showing that by removing the multilayer coating, the e_f values increase by 129% and 33% for the T5-U and T6R-U conditions, respectively.

3.4 Fractography

The coating surfaces of the T5-C (Figure 6(a)) and T6R-C (Figure 6(c)) samples show different morphology. T6R-C has a high crack density that increases close to the fracture surface (macroscopically visible circumferential cracks indicated by the arrow in Fig. 6(c)), where the high strain of the substrate leads to extensive delamination and fracture of the coating due to its lower ductility. In particular, considering the lower e_f and limited necking phenomena characterizing the T6R-C (Figure 6(c)) sample compared to the T6R-U (Figure 6(d)) one, the Ni-P interlayer acts as a highly brittle material and, once cracked under loading, transfers strain energy to the Al substrate due to the good adhesion (Figure 3), thus leading to a fast sample failure. The higher ductility of T6R-U compared to T6R-C is also evident by observing the smaller resistant area; even though the T6R heat treatment promotes a microstructural evolution, the lower ductility of the Ni-P interlayer leads to premature failure of the T6R-C sample

Both T5 samples (coated/uncoated) show no significant plastic deformation; however, they are characterized by different crack morphology. The T5-U (Figure 6(b)) has an inclined failure surface corresponding to the maximum shear stress planes (45° to the tensile axis). Conversely, the T5-C (Figure 6(a)) shows a fracture line perpendicular to the load direction and aligned with the circumferential detachment lines due to the compressive-tensile stress

condition at the substrate/coating interface [14]. The lower strain-bearing ability of the eutectic-Si network lead to material detachment along circumferential paths and incipient failure of the T5-C samples.

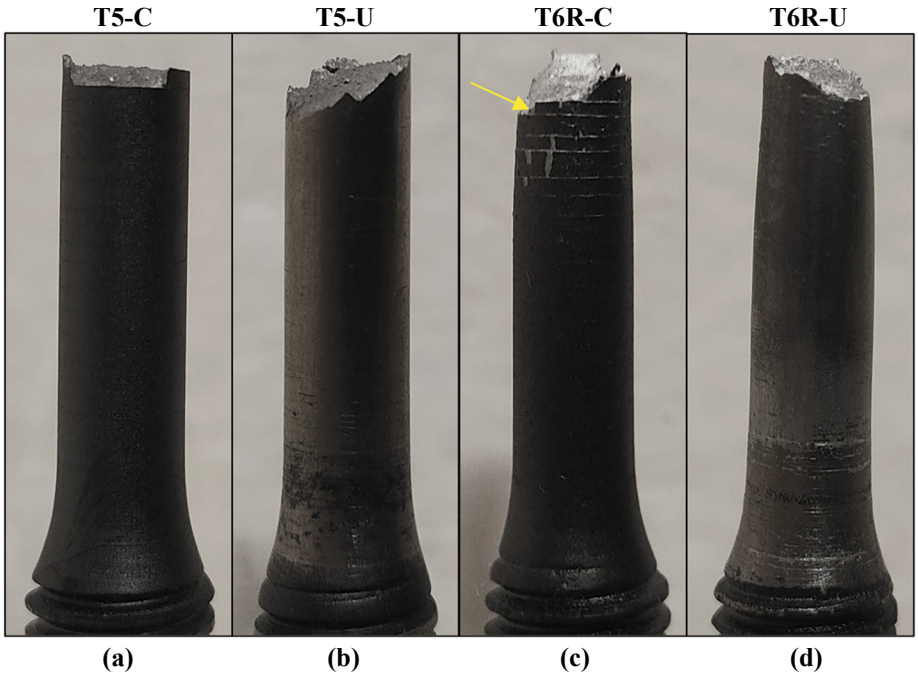

Fig. 6. State of the superficial coating and fracture morphology of the T5 and T6R alloy tested in different conditions: (i) coated (T5-C (a) and T6R-C (c)), (ii) uncoated (T5-U (b) and T6R-U (d)). The arrow in (c) points out macroscopically visible circumferential cracks.

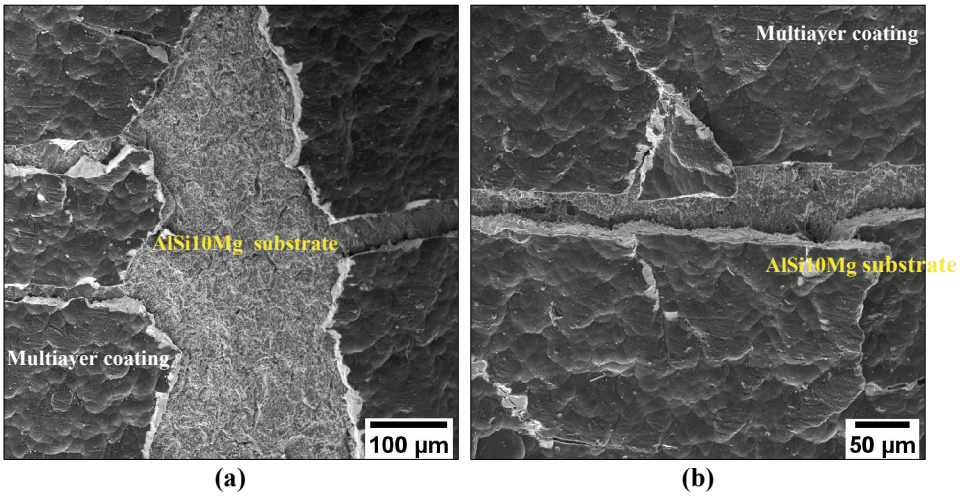

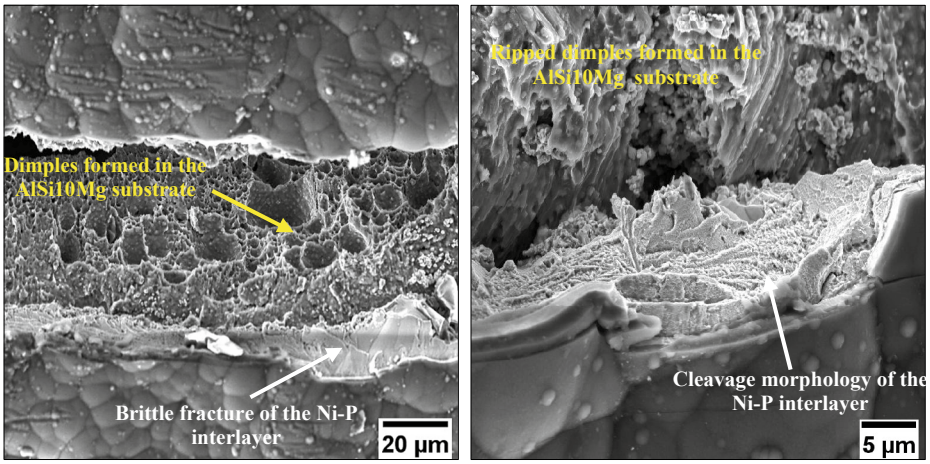

Fig. 7. T6R-C: fracture and detachment of the Ni-P interlayer from the substrate (a) (b). Different fracture mechanisms in the substrate (ductile) and Ni-P interlayer (brittle) (c,d). Ripped dimples formed in the AlSi10Mg substrate due to Ni-P interlayer delamination (d).

At high magnification, the multilayer coating on the T6R-C samples (Figure 7) is heavily cracked and extensively delaminated from the substrate, with wedge-shaped pieces tearing off during the tensile test (Figure 7(a,b)). In particular, Figures 7(c,d) show a Mode I crack opening for the Ni-P coating (with a typical dome-like surface morphology, fully replicated by the dark-grey DLC topcoat), characterized by flat faces and brittle fracture, while the Al substrate shows a ductile fracture morphology. During tensile loading, the load conditions induce circumferential compressive stresses in the coating and tensile stresses in the substrate [14], leading to debonding of Ni-P from the AlSi10Mg substrate. At room temperature, the deformation is inhomogeneous in amorphous materials (such as Ni-P and DLC) and almost entirely confined in intense shear bands [24]. Consequently, delamination phenomena may be associated with the shear stress at the substrate-Ni-P interface.

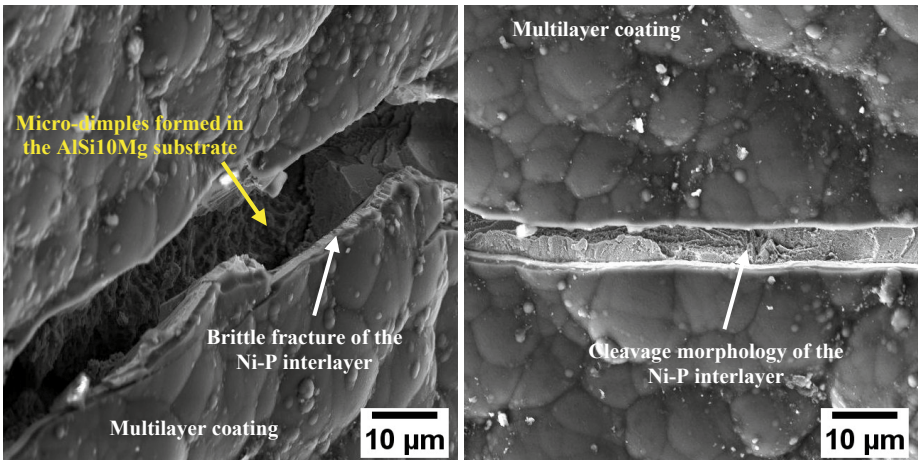

Fig. 8. Cracking of the multilayer coating close to the fracture surface of the T5-C sample (a,b). Different fracture mechanisms in the Al substrate (ductile) and Ni-P interlayer (brittle) are observable.

Conversely, T5 shows very light marks only close to the failure surface (Figure 8(a,b)). The interconnected eutectic-Si network of the T5 alloy is characterized by high load-bearing capacity and strain-hardening capability. However, the hard Si phase of the eutectic-Si network can not accommodate high strain before failure [21,25].

Therefore, the debonding at the Ni-P/substrate interface results from the compressive stresses developed in the coating due to the difference in the Poisson ratio and young's modulus between coating and substrate [14], which leads to a fast crack initiation and sample failure promoted by T5 microstructure.

Even though the Ni-P coating shows good overall adhesion to the L-PBF AlSi10Mg substrate (Figure 3), the higher Si phase density in T5 than in T6R (Fig. 4), as well as more capillary distribution and highly branched morphology of the eutectic-Si network, reduce the Ni-P substrate interface area and hence the adhesion of Ni-P to the substrate (Figure 9(a)). Conversely, the T6 composite-like microstructure provides a larger contact area between the Al matrix and the Ni-P coating, thus increasing both the adhesion and the ability of the coating to follow the plastic deformation of the substrate. This condition is highlighted by the fracture occurring within the substrate, a few microns underneath the Ni-P-substrate interface, with a layer of substrate material remaining well adherent to the Ni-P interlayer (Figure 9(b)).

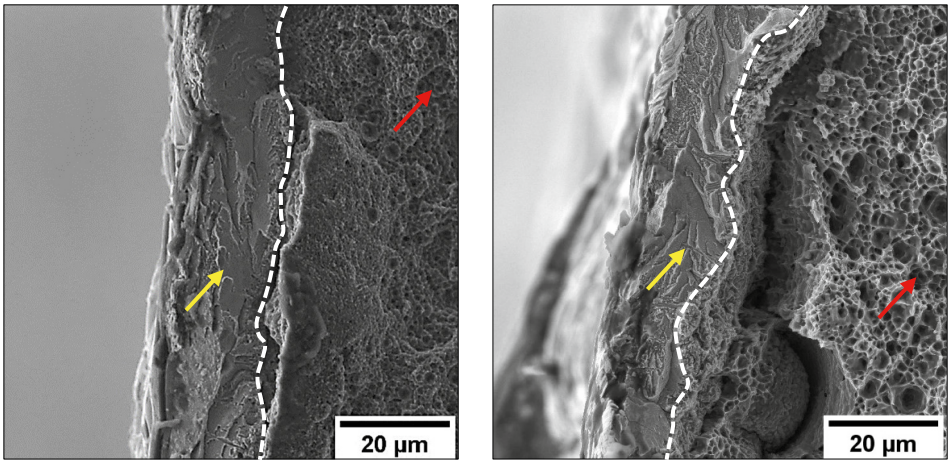

Fig. 9. High magnification of the fracture zone at the Al substrate/Ni-P coating interface of the T5-C (a) and T6R-C (b). Yellow arrows indicate chevron markings in the Ni-P interlayer typical of a brittle fracture. Red arrows point out submicrometric (a) and micrometric dimples (b). White dashed lines indicate the position of the substrate-Ni-P interface

Even though different e_f values characterize coated and uncoated samples, they show comparable failure mechanisms in the bulk material, mainly influenced by the heat treatment conditions. In particular, T5-C and T5-U samples (Figure 10(a,b)) show shallow dimples associated with the detachment of Al cells from the edges of the eutectic-Si network. Conversely, the T6-C and T6-U samples show a comparable ductile failure mode, characterized by deep dimples (Figure 10(c,d)) induced by the plastic deformation of the Al matrix around the Si particles.

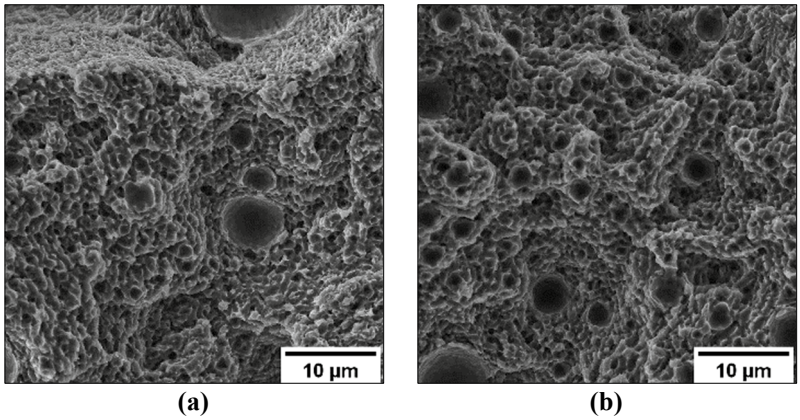

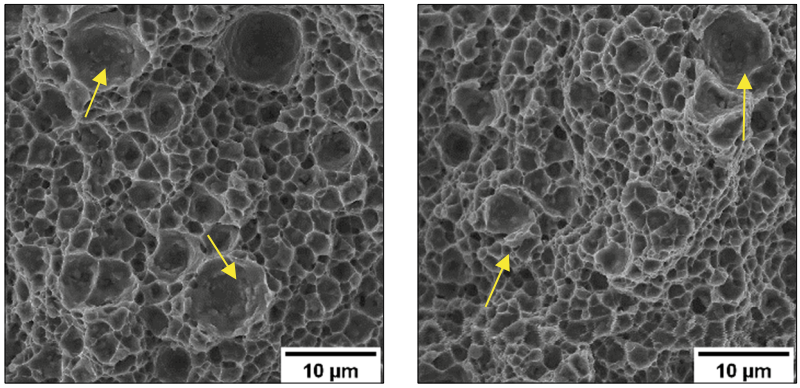

Fig. 10. Fracture morphologies of T5-C (a), T5-U (b), T6R-C (c), and T6R-U (d) samples. Yellow arrows indicate Si particles in (c) and (d).

4. Conclusions

This work investigated the influence of a Ni-9%P + DLC (a-C:H) multilayer coating on the tensile properties of the L-PBF AlSi10Mg alloy subjected to different integrated cycles: (i) Ni-P + DLC deposition (T5-like heat treatment) and (ii) SHT + Ni-P + DLC deposition (T6R-like heat treatment). Microstructural and mechanical characterizations were carried out to evaluate the effects of substituting artificial aging with DLC deposition. Failure mechanisms were analyzed to identify substrate and multilayer coating damage mechanisms. The following conclusions can be drawn:

- Integrating the heat treatment cycle in multilayer coating deposition does not induce significant microstructural modifications ;
- The multilayer coating increases the tensile properties of the T6R-like alloy (YS ≈ +4%, UTS ≈ +10%). Conversely, the UTS value of the T5-like alloy decreases by 12%;
- Uncoated samples (T5-U and T6R-U) have an e_f value of about 129% and 33% higher than coated samples, respectively, T5-C and T6R-C;
- Compressive/tensile stress condition at the Ni-P coating/substrate interface leads to coating cracking and delamination during tensile loading;
- The Ni-P interlayer shows a higher adhesion on the T6 composite-like microstructure compared to the microstructure with a continuous eutectic-Si network of the T5-like one;
- The multilayer coating does not modify the main fracture mechanisms of the heat-treated substrate.

In conclusion, the variation in the tensile property balance of the L-PBF AlSi10Mg alloy reveals some critical points that should be considered when applying a multilayer coating to structural components. However, integrated cycle conditions (i.e., the above-described T5-like and T6R-like cycles, where coating deposition contributes to heat treatment) can result in a good compromise between technological and mechanical requirements. Further analyses, such as fatigue tests, will be carried out to validate this solution.

References

1. Altıparmak, S.C., Yardley, V.A., Shi, Z., Lin, J., 2021. Challenges in additive manufacturing of high-strength aluminium alloys and current developments in hybrid additive manufacturing. International Journal of Lightweight Materials and Manufacture, 4(2), 246-261.
2. Rometsch, P.A., Zhu, Y., Wu, X., Huang, A., 2022. Review of high-strength aluminium alloys for additive manufacturing by laser powder bed fusion. Materials & Design, 219, 110779.

3. Shakil, S.I., Hadadzadeh, A., Shalchi Amirkhiz, B., Pirgazi, H., Mohammadi, M., Haghshenas, M., 2021. Additive manufactured versus cast AlSi10Mg alloy: Microstructure and micromechanics. Results in Materials, 10, 100178.
4. Puchi-Cabrera, E.S., Villalobos-Gutiérrez, C., Irausquín, I., La Barbera-Sosa, J., Mesmacque, G., 2006. Fatigue behavior of a 7075-T6 aluminum alloy coated with an electroless Ni–P deposit. International Journal of Fatigue, 28(12), 1854-1866.
5. Wang, Y., Tung, S.C., 1999. Scuffing and wear behavior of aluminum piston skirt coatings against aluminum cylinder bore. Wear, 225-229(2), 1100-1108.
6. Teng, D., Wang, J., Li, C., Sa, X., 2022. Investigation of Friction and Wear Behavior of Cast Aluminum Alloy Piston Skirt with Graphite Coating Using a Designed Piston Skirt Test Apparatus. Materials, 15, 4010.
7. Staia, M.H., Puchi Cabrera, E.S., Iost, A., Zairi, A., Belayer, S., Van Gorp, A., 2015. Tribological response of AA 2024-T3 aluminium alloy coated with a DLC duplex coating. Tribology International, 85, 74-87.
8. Donnet, C. and Erdemir, A. (eds.) (2008). Tribology of Diamond-Like Carbon Films. Boston, MA: Springer.
9. Lee, C.K., Chen, C.H., Tan C.A., 2016. Electrochemical corrosion and wear behavior of an ultra-thin DLC film deposited on different annealing Ni-P layers on Al-Mg alloy in NaCl solution. Int. J. Electrochem. Sci., 11, 5983-5998.
10. Maruno, H., Nishimoto, A., 2018. Adhesion and durability of multi-interlayered diamond-like carbon films deposited on aluminum alloy. Surface and Coatings Technology. 354, 134-144.
11. Salicio-Paz, A., Grande, H., Pellicer, E., Sort, J., Fornell, J., Offoiach, R., Lekka, M., García-Lecina, E., 2019. Monolayered versus multilayered electroless NiP coatings: Impact of the plating approach on the microstructure, mechanical and corrosion properties of the coatings. Surface and Coatings Technology, 368, 138-146.
12. Rahmat, M.A., Oskouei, R.H., Ibrahim, R.N., Singh Raman, R.K., 2013. The effect of electroless Ni–P coatings on the fatigue life of Al 7075-T6 fastener holes with symmetrical slits, International Journal of Fatigue, 52, 30-38.
13. Mohan Kumar, S., Pramod, R., Shashi Kumar, M.E., Govindaraju, H.K., 2014. Evaluation of Fracture Toughness and Mechanical Properties of Aluminum Alloy 7075, T6 with Nickel Coating, Procedia Engineering, 97, 178-185.
14. Bouaziz, H., Brinza, O., Haddar, N., Gasperini, M., Feki, M., 2017. In-situ SEM study of crack initiation, propagation and interfacial debonding of Ni-P coating during tensile tests: Heat treatment effect. Materials Characterization, 123, 106-114.
15. Di Egidio, G., Ceschini, L., Morri, A., Martini, M., Merlin, M., 2022. A Novel T6 Rapid Heat Treatment for AlSi10Mg Alloy Produced by Laser-Based Powder Bed Fusion: Comparison with T5 and Conventional T6 Heat Treatments. Metallurgical Material Transactions B, 53, 284–303.
16. Di Egidio, G.; Ceschini, L.; Morri, A.; Zanni, M. Room- and High-Temperature Fatigue Strength of the T5 and Rapid T6 Heat-Treated AlSi10Mg Alloy Produced by Laser-Based Powder Bed Fusion. Metals 2023, 13, 263.
17. Parkinson, R. Properties and applications of electroless nickel. Vol. 37. Toronto: Nickel Development Institute, 1997.
18. Krishnan K et al. An overall aspect of electroless Ni–P depositions—a review article. Metall Mater Trans A 2006;37(6):1917–2
19. Di Egidio, G; Morri, A.; Ceschini L.; Tonelli L. High-Temperature Behavior of the Heat-Treated and Overaged AlSi10Mg Alloy Produced by Laser-Based Powder Bed Fusion and Comparison with Conventional Al–Si–Mg-Casting Alloys. Adv. Eng. Mater. 2023, 2201238.
20. Y. Garcés, H. Sánchez, J. Berríos, A. Pertuz, J. Chitty, H. Hintermann, E.S. Puchi, Fatigue behavior of a quenched and tempered AISI 4340 steel coated with an electroless Ni-P deposit, Thin Solid Films, Volumes 355–356, 1999, Pages 487-493, https://doi.org/10.1016/S0040-6090(99)00673-2
21. Delahaye, J.; Tchuindjang T.; Lecomte-Beckers, J.; Rigo, O.; Habraken, A.M.; Mertens, M. Influence of Si precipitates on fracture mechanisms of AlSi10Mg parts processed by Selective Laser Melting, Acta Mater. 2019, 175, 160-170.
22. Prasanta Sahoo, Suman Kalyan Das, Tribology of electroless nickel coatings – A review, Materials & Design, Volume 32, Issue 4, 2011, Pages 1760-1775, ISSN 0261-3069, https://doi.org/10.1016/j.matdes.2010.11.013.
23. Krishnan K et al. An overall aspect of electroless Ni–P depositions—a review article. Metall Mater Trans A 2006;37(6):1917–2
24. Panagopoulos, C.N., Papachristos, V.D. & Sigalas, C. Tensile behaviour of as deposited and heat-treated electroless Ni-P deposits. Journal of Materials Science 34, 2587–2600 (1999). https://doi.org/10.1023/A:1004600732400
25. Chen, S.; Tan, Q.; Gao, W.; Wu, G.; Fan, J.; Feng, Z.; Huang, T.; Godfrey, A.W.; Zhang, M.; Huang, X. Effect of heat treatment on the anisotropy in mechanical properties of selective laser melted AlSi10Mg, Mater. Sci. Eng., A 2022, 858, 144130.